Talanta 83 (2011) 1023–1029

Contents lists available at ScienceDirect

Talanta

journal homepage: www.elsevier.com/locate/talanta

Ordered gold nanoparticle arrays as surface-enhanced Raman spectroscopy substrates for label-free detection of nitroexplosives

Xiaojuan Liu[a,c], Liang Zhao[b,c], Hao Shen[b,c], Hongxing Xu[b], Lehui Lu[a,*]

[a] State Key Laboratory of Electroanalytical Chemistry, Changchun Institute of Applied Chemistry, Chinese Academy of Science, 5625 Renmin Street, Changchun Jilin 130022, PR China
[b] Beijing National Laboratory for Condensed Matter Physics, Institute of Physics, Chinese Academy of Sciences, Beijing 100190, PR China
[c] Graduate School of the Chinese Academy of Sciences, Beijing 100039, PR China

ARTICLE INFO

Article history:
Received 11 August 2010
Received in revised form 29 October 2010
Accepted 4 November 2010
Available online 11 November 2010

Keywords:
2,4,6-Trinitrotoluene detection
Self-assembly
Ordered gold nanostructure
SERS

ABSTRACT

Nitroexplosives, such as 2,4,6-trinitrotoluene (TNT) which is a leading example of nitroaromatic explosives, are causing wide concern. Motivated by the urgent demand for trace analysis of explosives, novel surface-enhanced Raman spectroscopy substrates based upon highly ordered Au nanoparticles have been fabricated by a simple droplet evaporation method. It is noteworthy that an ethylhexadecyldimethyl ammonium bromide bilayer surrounding each individual nanoparticle not only is responsible for these periodic gap structures, but also tends to promote the adsorption of TNT on the composite NPs, thus resulting in a considerable increase of Raman signal. These desirable features endow the resulting SERS substrates with excellent enhancement ability and allow for a label-free detection of common plastic explosive materials even with a concentration as low as 10^{-9} M.

© 2010 Elsevier B.V. All rights reserved.

1. Introduction

Detection of nitroexplosives has attracted more and more attention in recent years owing to homeland security, environmental and humanitarian implications. 2,4,6-Trinitrotoluene (TNT), which has significant detrimental effects on the environment and human health, is one of the most commonly used nitrated explosives in the preparation of landmines for military and terrorist activities [1]. The presence of TNT is directly correlated with criminal intent or the presence of ordinances such as unexploded land mines or cluster bombs. As a result, it is important to develop highly sensitive, cost-effective sensors that can provide real-time determination of TNT level in the environment. In recent years, a variety of sensors for analyzing TNT have been developed. These include the followings: (1) fluorescent sensors, which were based on the fact that fluorescent organic polymers [2,3] or fluorescent silicon NPs [4] and so on [5,6] can be quenched by nitroaromatic explosives; (2) colorimetric sensors, which were developed on the basis of the aggregation of functionalized AuNPs in the presence of TNT [7]; (3) voltammetric sensors, which were based on the electrochemical activity of the nitro groups of TNT [8–10]; (4) biosensors, such as antibody-based optical [11,12] or microgravimetric quartz-crystal-microbalance biosensors [13]; (5) spectroscopic sensors that can detect explosives using surface-enhanced Raman spectroscopy [14–16]. Among them, spectroscopic sensors based on SERS have attracted much attention from the perspectives of both fundamental understanding and practical applications.

Surface-enhanced Raman scattering (SERS) is a powerful analytical technique that allows ultra-sensitive chemical or biochemical analysis [17,18], because it can result in a dramatic increase in Raman signals from molecules that have been absorbed onto or are in the vicinity of nanometer-sized metallic particles [19]. The high Raman enhancement was attributed to electromagnetic and chemical enhancement mechanisms [20]. It has been generally accepted that SERS is dominated by strong electromagnetic field enhancement near metallic nanostructures, and that surface plasmon coupling at the junctions or gaps between these structures creates 'hot spots' with the enormous enhancement necessary for high-sensitivity SERS detection [21–25]. Its high sensitivity has been extended to the single-molecule level. In addition to sensitivity, another important feature of SERS is the level of detection specificity that can be achieved by controlling the chemistry around the metal surface. A specific chemical moiety can be incorporated on the surface of the SERS substrates to target the detection of a single species present in a complex sample mixture at trace levels (*e.g.*, submicromolar) without having to physically separate out interfering species [26]. Raman signals can yield unique vibrational signatures of analytes associated with chemical and structural information without interference from the capping agents of the metal nanoparticles [27]. Moreover, compared to fluorescence peaks, most Raman bands are ~100 times narrower, which further reduce spectral overlap and screen. Also, photobleaching is much

* Corresponding author. Tel.: +86 431 85262418; fax: +86 431 85262406.
E-mail address: lehuilu@ciac.jl.cn (L. Lu).

0039-9140/$ – see front matter © 2010 Elsevier B.V. All rights reserved.
doi:10.1016/j.talanta.2010.11.015

less severe with Raman signals thus enabling lower detection limits and better repeatability [28].

From the application viewpoint of SERS technology, metal nanostructures, which can provide the largest enhancement, must be produced. The major requirements for the SERS substrate materials include controlled nanoscale structure, periodicity and chemical stability [29,30]. Our previous studies showed that highly ordered metal nanostructures had good SERS enhancement properties [31–34]. And a number of approaches for fabrication of closely packed nanostructure arrays have been explored including electron beam lithography [35], nanosphere lithography [36] and focused ion beam milling [37]. However, most of them are too technologically demanding and expensive to be used to fabricate large quantities of substrates for practical applications. Recently, our group reported the strategies for the fabrication of large-area silver-coated silicon nanowire arrays [38] and uniform silver-coated ZnO nanowire arrays [39]. It was found that the as-prepared silver-coated silicon nanowire arrays possess excellent SERS enhancement ability and good reproducibility. The silver-coated ZnO nanowire arrays exhibited high catalytic activity and good SERS performance, which provided an excellent platform for monitoring the catalytic degradation of dye molecules by SERS technology. Nevertheless, the complicate experimental procedures are big challenge for their practical applications. In comparison to the above-mentioned methods, a simple strategy for the preparation of periodic nanoparticle arrays has been published by Halas and co-workers [40]. They have elegantly demonstrated that CTAB-coated gold nanoparticles can be drop-cast onto indium doped tin oxide (ITO) glass slides to produce hexagonally close-packed monolayer of AuNPs arrays. This self-assembly strategy has been one of the most popular methods for SERS applications because of its simple procedure. Another advantage is the preparation of extremely narrow interparticle gaps, providing a large SERS enhancement factor of 10^8 for pMA which is close to the theoretical calculation for the perfect Au nanosphere array [41].

Herein, we report our attempt to utilize a simple droplet evaporation process to assemble highly ordered Au octahedral arrays with nanoscale interparticle gaps. The resulting AuNPs arrays can serve as good surface-enhanced Raman spectroscopy (SERS) substrates, which can provide exceptionally strong enhancement in Raman scattering for ultrasensitive detection of TNT. Gold octahedra with an edge length of about 42 nm were prepared according to a seed-mediated growth approach in the presence of an aqueous ethylhexadecyldimethyl ammonium bromide (EHDAB) as the capping agent, which can form a bilayer structure around the gold surface [42]. Such bilayer structure leads to a positive charge on the NPs surfaces, providing a net repulsive interaction between the NPs to prevent random disordered aggregation and hence form quite densely packed but separated with nanometer interparticle gaps during solvent evaporation [43]. Compared with the disordered gold structure as well as the bare ordered gold structure, these periodic arrays of EHDAB-coated gold nanoparticles exhibit distinct advantages toward the detection of TNT in terms of sensitivity and reproducibility.

2. Experimental

2.1. Chemicals and materials

All chemical regents were obtained from commercial suppliers and used without further purification. Sodium borohydride ($NaBH_4$), ethylhexadecyldimethyl ammonium bromide (EHDAB), ascorbic acid were purchased from Sigma–Aldrich. Gold chloride trihydrate ($HAuCl_4{\cdot}3H_2O$) was purchased from Alfa Aesar. Deionized water (resistance >18.2 $M\Omega\,cm^{-1}$) was used throughout the experiments.

2.2. Preparation of gold octahedra

Gold octahedra were prepared according to a seed-mediated growth in aqueous solutions [43,44], which have been used widely for the preparation of Au nanostructures. Specifically, the seeds were prepared by the reduction of $HAuCl_4$ (0.01 M, 0.25 mL) by ice-cold $NaBH_4$ (0.01 M, 0.6 mL) in the presence of EHDAB (0.1 M, 7.5 mL). The $NaBH_4$ solution was added at a time to the solution containing EHDAB and $HAuCl_4$, and the reaction mixture was then magnetically stirred for 2 min. The resultant seed solution was kept at room temperature for 1 h before use. The growth solution was prepared by the sequential addition of EHDAB (0.1 M, 6.4 mL), $HAuCl_4$ (0.01 M, 0.75 mL), and ascorbic acid (0.1 M, 3.8 mL) into water (32 mL). The EHDAB-stabilized seed solution was diluted 10 times with water. The diluted seed solution (0.06 mL) was then added into the growth solution for the growth of Au octahedra. The resulting solution was mixed by gentle inversion for 10 s and then left undisturbed overnight. The as-grown octahedra were washed twice by centrifugation and condensed into a final volume of about 1 mL for further application.

2.3. Fabrication of Au octahedral arrays

The solid substrate was cleaned by sequential ultrasonication in acetone, ethanol, deionized water for 15 min in each and then treated with H_2SO_4/H_2O_2 (3:1 (v/v) H_2SO_4 (97%)/H_2O_2 (30%)) at 80 °C for 30 min to derive a hydroxyl surface. After thorough rinsing with Milli-Q ultrapure water, the cleaned silicon wafer was dried in air. For the preparation of Au nanostructure assemblies, a drop (10 μL) of the concentrated of Au nanostructures was placed onto the silicon substrate. The sessile droplet was kept still for evaporation of water under ambient conditions. For TNT sensing, 10 μL of TNT solution in ethanol with different concentrations was placed on the Raman substrates and was dried at room temperature.

2.4. Characterization

SEM images were taken with a FEI/Philips XL30 ESEM FEG field-emission scanning electron microscope operating at an acceleration voltage of 20 kV. Transmission electron microscope (TEM) images were obtained using a JEOL 2000 transmission electron microscope operating at 100 kV. XRD data were collected on a D/Max 2500 V/PC X-ray diffractometer with a Cu Kα X-ray radiation source. UV–vis absorption spectra were recorded on a Varian Cary 500 UV–Vis-NIR spectrometer. SERS spectra were obtained using a Renishaw in Via micro Raman spectroscopy system. The 632.8 nm radiation from a HeNe laser was used as the excitation source. The laser beam was focused on a spot with a diameter of approximately 1 μm using a 50× microscope objective. The data acquisition time was 10 s for one accumulation. The Raman band of a silicon wafer at 520 cm^{-1} was used to calibrate the spectrometer.

3. Results and discussion

3.1. Fabrication of highly ordered Au octahedral arrays

Gold octahedra with an edge length of about 42 nm were used as building blocks of 2D and 3D superlattics, because previous studies showed that noble metal nanoparticles exhibit size- and shape-dependent SERS properties [45]. In terms of geometrical effect, the strongest SERS effect has been determined for nanoparticles having sharp features which have more well-defined corners and edges, facilitating the induction of intense near-field enhancements localized around these sharp surface features [46]. Furthermore, the controlled fabrication of highly regular metallic nanostructure

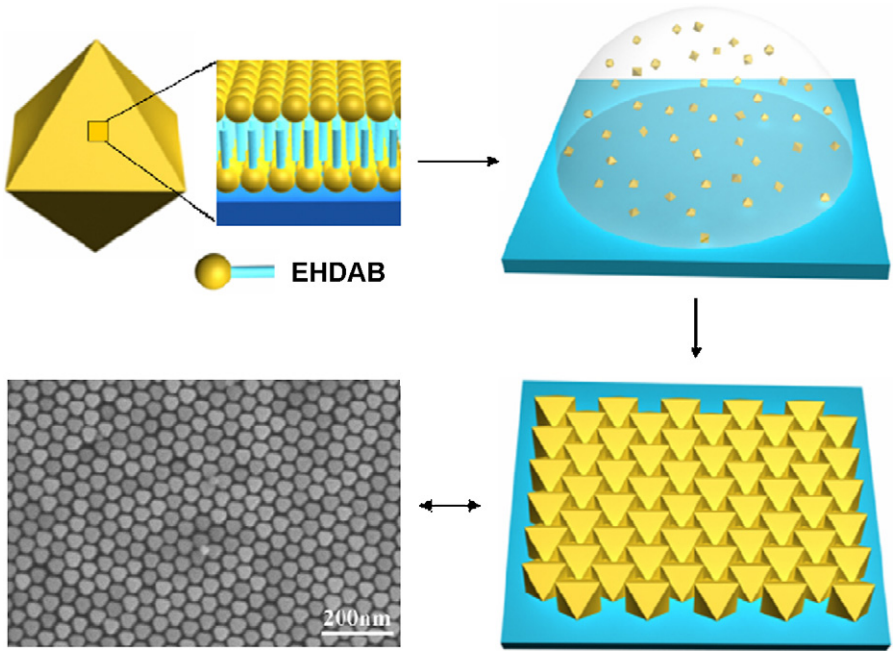

Fig. 1. Schematic showing an Au octahedron stabilized by an ethylhexadecyldimethyl ammonium bromide (EHDAB) bilayer, and droplet-evaporation technique that can induce the formation of ordered AuNPs superstructures.

geometries with a high density of sub-10-nm interparticle spacing was also important for high-performance SERS-based sensors. Fig. 1 schematically illustrates the fabrication procedure for highly ordered nanostructured arrays. In this approach, colloidal dispersions of shaped gold nanoparticles spontaneously adopt ordered structures with slow sedimentation and subsequent solvent evaporation under ambient conditions [47]. The assembly mechanism of EHDAB-protected gold octahedra was believed to be a result of the interplay of capillary and interfacial forces [48]. With this strategy, both 2D and 3D well-ordered assemblies of gold nanostructures were obtained and successfully applied for the SERS measurements.

3.2. Structural characterization

The microstructure of the samples was investigated using scanning electron microscopy (SEM). Fig. 2A shows the SEM image of the as-prepared sample produced by droplet evaporation. As can be observed, all the products are composed of a large quantity of homogeneous nanoparticles with a well-defined octahedral shape. Moreover, the gold octahedra assemble into hexagonally close-packed monolayer of EHDAB-coated AuNPs. The interparticle distance of the prepared 2D ordered arrays have an average interparticle distance of $\sim 6 \pm 2$ nm, which correlate well to the thickness of two adjacent EHDAB bilayers, each with a thickness of 3.2 nm [49].

The crystal structure of the gold nanoparticles was also characterized by TEM and XRD measurement. Representative TEM image of the gold nanoparticles used for the assembly is shown in Fig. 2B. Many octahedron nanoparticles can be easily identified in this sample. While TEM and SEM often sample only a small portion of the products, X-ray diffraction (XRD) can be used to assess the overall quality and purity of the facetted gold nanoparticles. Fig. 2C shows the corresponding XRD pattern of the freshly prepared octahedral gold nanoparticles. From the XRD pattern, five peaks are observed and all the diffraction peaks can be indexed to face-centered cubic (fcc) structure of metal gold (JCPDS No. 04-0784). The peaks located at $2\theta = 38.16^\circ$, 44.34°, 64.59°, 77.55° and 81.73° are assigned to the (1 1 1), (2 0 0), (2 2 0), (3 1 1) and (2 2 2) reflections, respectively. The intensity ratio between the (2 0 0) and (1 1 1) diffraction peaks is 0.022, which is significantly smaller than the conventional bulk intensity ratio ($\approx$0.53). This result suggests that the faces of these nanoparticles were primarily composed of (1 1 1) planes, and thus their (1 1 1) planes tended to preferentially orient parallel to the surface of the supporting substrate [50,51]. Gold nanocrystals normally show very intense color due to surface plasmon resonance (SPR) scattering, which is highly dependent on the size and shape of the particles. Fig. 2D shows the UV–vis spectrum of the AuNPs aqueous solution, in which a SPR band is observed at 557 nm.

We were intrigued by the fact that 3D SERS substrates offer large specific surface area for the adsorption of target analytes and provide a large density of hot spots within the laser-illumination area [52]. Therefore, multilayered nanoparticle films with intralayer and interlayer coupling of plasmon resonances were fabricated using more concentrated AuNPs colloid. When a more concentrated AuNPs colloid was drop cast on a silicon wafer, the subsequent deposition of gold octahedra typically resulted in formation of increased proportion of multilayer structures in the observed regions. It is well known that homogeneity of size and shape are essential to obtain well-ordered close packed superstructures using the droplet-evaporation technique. In this case, the top (Fig. 3A) and lateral face (Fig. 3B) view SEM images of the 3D superstructure reveal that Au octahedra assemble into highly ordered structures within each layer. Besides, the formation of such structure is a complicated process where different driving force may be involved, such as entropy, Coulomb interaction from particle charges, London-van der Waals forces, charge–dipole interaction, and dipole–dipole interactions. Therefore, the formation mechanism has been not yet well understood.

3.3. SERS properties

To evaluate the SERS performance of the SERS substrates that were fabricated using concentrated AuNPs colloid, 4-aminothiophenol (ATP) was chosen as the model molecule because thiolated compounds have been shown to effectively displace EHDAB from gold nanoparticles due to the stronger Au–S bond

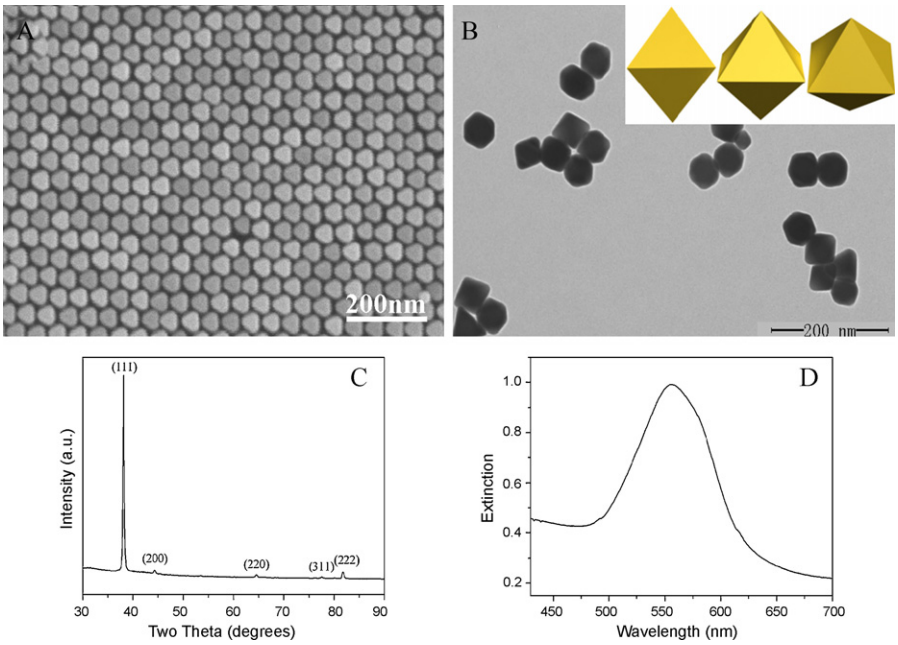

Fig. 2. (A) Typical SEM image of the hexagonally close-packed monolayer of Au polyhedra arrays; (B) representative TEM image of the gold nanoparticles used for the assembly, the same octahedron seen in different views is shown in inset; (C) XRD pattern of the freshly prepared octahedral gold nanoparticles; (D) UV–vis absorption spectrum of the AuNPs aqueous solution.

relative to Au–Br [53]. Fig. 4 compares the SERS spectra of ATP molecules obtained from the highly ordered nanoparticle arrays and the AuNPs with disordered structures. SERS signals are observed in both cases, but it is evident that the ordered arrays exhibit the higher enhancement efficiency at 633 nm excitation (Fig. 4). It is well known that SERS enhancement results from an intense local amplification of the electric field near a metal surface when collective oscillations of conduction electrons resonate in phase with the incident light. The electromagnetic interaction (electromagnetic coupling) between metal nanostructures greatly increases the SERS intensity, thus directly influencing the degree of Raman enhancement exhibited. In fact, almost all SERS-active systems are composed of interacting metal nanoparticles arranged in close proximity to each other [52]. As stated above, the SERS substrate prepared by droplet evaporation technique is composed of close-packed gold nanoparticles. When excited by incident light, the collective surface plasmons are localized at these close-packed gold nanoparticles, leading to the formation of a local field in this region. The localized resonant plasmon modes can contribute to larger SERS enhancement [54,55].

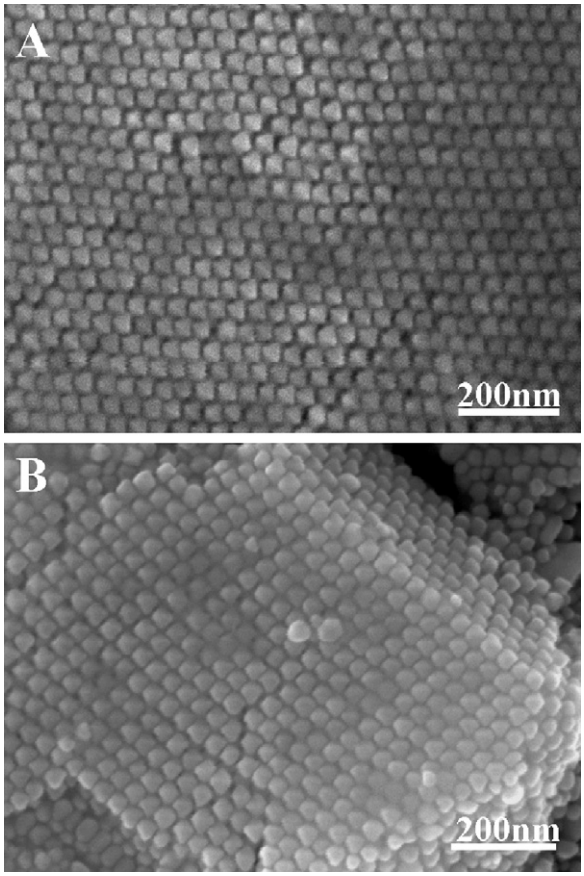

Fig. 3. SEM images of the highly ordered multilayer Au octahedra.

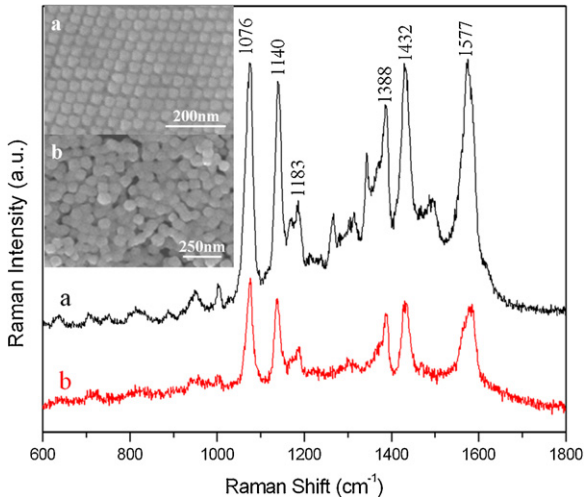

Fig. 4. SERS spectra of 100 μM 4-aminothiophenol (4-ATP) absorbed on (a) highly ordered nanoparticles arrays (633 nm, 430 μW), (b) disordered structures (633 nm, 845 μW). The inset shows the representative SEM images.

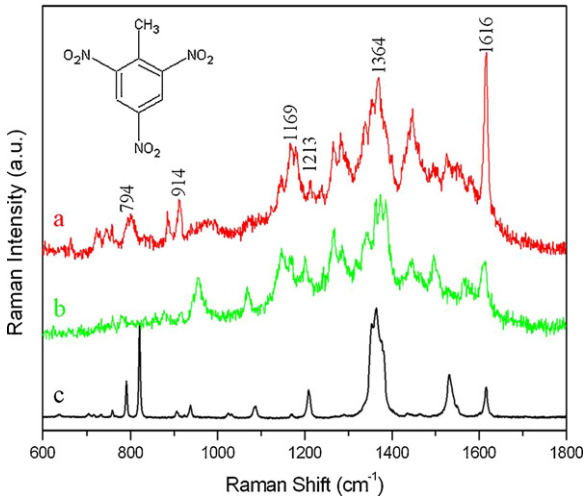

Fig. 5. SERS spectra of TNT (the inset shows its structure) with different concentrations on the SERS substrates: (a) 10^{-8} M, (b) 10^{-9} M; (c) Raman spectra of TNT on silicon wafer. The spectra were recorded using 88 μW (a, b) and 2 mW (c) of 633 nm laser light.

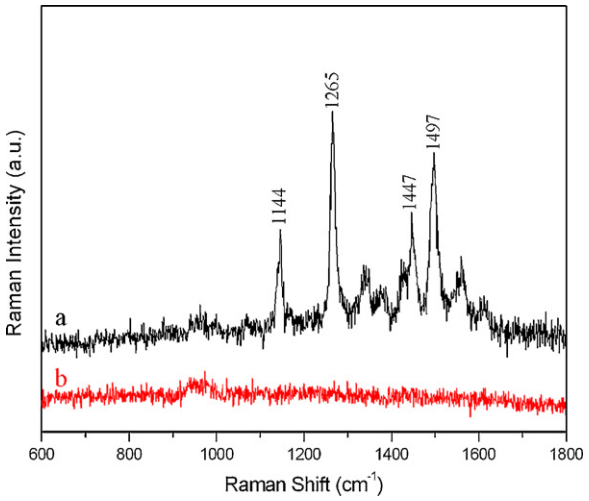

Fig. 6. SERS spectra acquired from EHDAB-coated gold nanoparticle arrays on silicon wafer before (a) and after (b) O_2 plasma etching. Laser wavelength 633 nm, excitation intensity 88 μW.

3.4. Application

The observed large enhancement suggested that the highly ordered gold octahedra arrays can indeed serve as robust solid substrates for carrying out molecular sensing with high sensitivity and specificity. To demonstrate that they may find further applications in human health and safety, we selected 2,4,6-trinitrotoluene (TNT), a high explosive, as the target molecule. The neat (Fig. 5c) and SERS spectra (Fig. 5a, b) show the same features with minor shifts to the frequencies of some bands but also significant enhancement is observed particularly for modes at 1616, 1364 cm^{-1} and a weaker feature (1167 cm^{-1}) all corresponding to TNT. Although the background spectrum from the substrate contains features from EHDAB, these SERS signals cannot overlap and screen those corresponding to the analyte.

On the basis of previous reports [14–16,56], the observed Raman and SERS peaks have been assigned. The peak at 1616 cm^{-1} is attributed to the C=C aromatic stretching vibration. The strong Raman band at 1364 cm^{-1} is due to the NO_2 symmetric stretching vibration. The peak at 1213 cm^{-1} comes from the vibration of the C_6H_2–C bonds. The peak around 1169 cm^{-1} is contributed form C–C (ring) in plane trigonal bend and 2,4,6 C–N stretch. The peak at 914 cm^{-1} is mainly from C–N stretching vibration. The peak at 790 cm^{-1} arises from C–H out-of-plane bend. All of them are due to TNT vibration. As compared to Fig. 6a, other observed Raman bands in Fig. 5a, b such as 1144, 1265, 1447, 1497 cm^{-1} arising from EHDAB which coated gold nanoparticles on silicon substrate. The signature stretching modes at 1364 cm^{-1} and 1616 cm^{-1} were utilized to detect the presence of TNT compound at very low concentrations (Fig. 5a, b). As was observed, the peaks at 1364 cm^{-1} and 1616 cm^{-1} are clearly visible down to 1 nM. It is worth noting that the signal-to-noise ratio of the peaks at 1616 and 1364 cm^{-1} is larger than 3. In addition, compared to previous reports [14–16], an extremely low incident laser power (in the μW range) was used in order to minimize heating and photochemical effects during SERS measurements and the acquisition time was 10 s.

It is noteworthy that cationic stabilizing surfactants used in this case play an important role not only in the formation of ordered nanoparticle superstructures by droplet evaporation, but also in the adsorption of TNT on the gold nanoparticles surface. The effect of EHDAB on the adsorption of TNT was investigated. Plasma treatment [57] was carried out to remove EHDAB molecules adsorbed on the surface of the Au octahedra. Fig. 6 illustrates spectra of bilayer protected gold nanoparticle arrays on silicon before and after plasma etching. After the sample had been plasma etched for 1 min, all of the EHDAB peaks (in curve a) disappeared from the SERS spectrum (curve b), indicating complete removal of the EHDAB molecules from the surface of the octahedron. To evaluate the sensitivity of the above-mentioned substrates, a drop of 10^{-8} M TNT solution in ethanol was put on the Raman substrates and was dried at room temperature. The resulted spectra are shown in Fig. 7. It was found that as-prepared EHDAB-coated highly ordered Au octahedra arrays possess the higher sensitivity. Whereas the plasma treated sample gives only a very weak enhancement. It is important to note that SERS effect has been attributed to an enhancement in the scattering efficiencies that occur for molecules localized near nanostructured metal surfaces, so the observed different sensitivity is likely owing to the reasons that are considered as follows. The affinity of the functional groups in the TNT toward colloidal gold surfaces is very low, and it is the affinity which determines the analytes retention on the metal surfaces. Thus, TNT does not adsorb efficiently on the bare gold surfaces. In comparison to a bare gold surface, the capping molecules on the surface of the gold layer tend

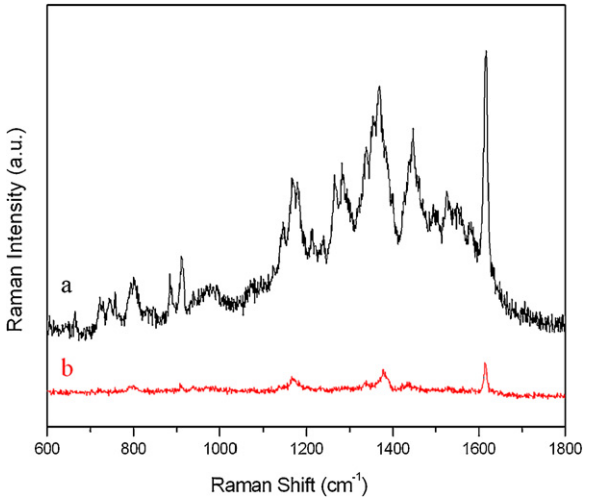

Fig. 7. SERS spectra of 10^{-8} M TNT on different SERS substrates: (a) EHDAB bilayer protected gold nanoparticles arrays; (b) plasma treated sample. The spectra were recorded using 88 μW of 633 nm laser light.

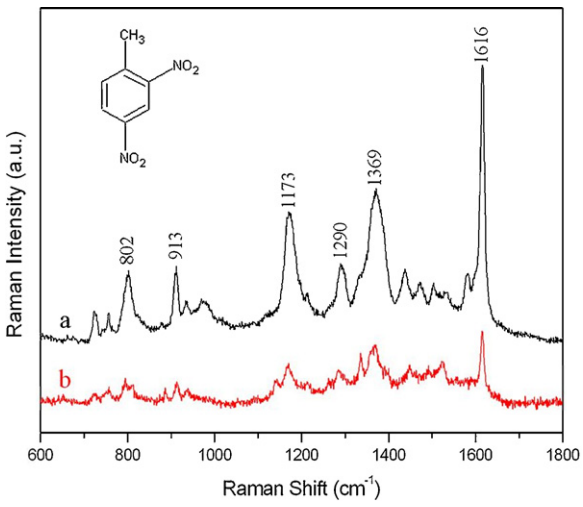

Fig. 8. SERS spectra of DNT (the inset shows its structure) with different concentrations on the SERS substrates: (a) 10^{-6} M, (b) 10^{-8} M, measured with a 633 nm (88 μW) laser line.

to increase the total number of analyte molecules in the proximity of the gold surface. Moreover, these TNT molecules are expected to be able to penetrate into the hot-spot region between the closely spaced particles owing to their relatively small sizes.

In addition, we tried to clarify if the substrates suggested here can be expandable to other small organic molecules from a common explosive list, we explored the possibility of directly detecting 2,4-dinitrotoluene (DNT) molecule, which is often used as a model nitroaromatic compound for TNT-based plastic explosives. Fig. 8 shows the SERS spectrum of 10^{-6} and 10^{-8} M DNT molecules obtained from the highly ordered EHDAB-capped Au NPs arrays. The NO_2 stretching mode at 1369 cm^{-1} and the C=C aromatic stretching vibration at 1616 cm^{-1}, which are the main vibrational modes for the analysis of 2,4-DNT, are clearly displayed and well-separated from the surfactant-related Raman bands. It is evident that SERS spectrum of DNT is still discernable even at a concentration of 10^{-8} M, which enables SERS-based ultra-sensitive detection of DNT.

However, a useful SERS substrate must be able to discriminate analytes from common interferents in ambient environment. Thus, we performed further experiments testing the response of the SERS substrate to other nitro compounds, such as 2-nitrotoluene, nitrobenzene, nitroethane, all of which are non-explosive in nature (Fig. 9). Remarkably, each of these molecules exhibits its own Raman fingerprint character, which is evidently distinguished from that of TNT. For example, the peaks at 794, 914, and 1616 cm^{-1} are the characteristic vibrational patterns of TNT, which are absent from the SERS spectra of the other three molecules. These results clearly show excellent selectivity of the substrate over other non-explosive nitro compounds.

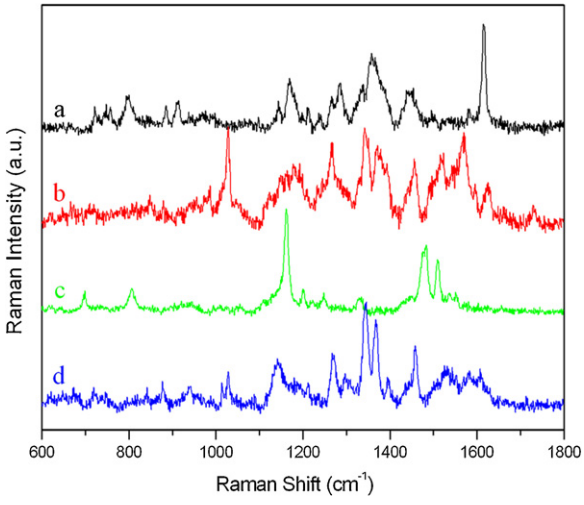

Fig. 9. SERS spectra of (a) 10^{-8} M TNT, (b) 10^{-7} M 2-nitrotoluene, (c) 10^{-7} M nitrobenzene, and (d) 10^{-6} M nitroethane on the SERS substrates. The spectra were recorded using 88 μW of 633 nm laser light.

4. Conclusions

In summary, we have demonstrated the fabrication of highly ordered Au octahedra arrays by droplet evaporation. The resultant ordered gold nanostructures can be used as SERS substrates exhibiting excellent enhancement ability. These highly active substrates allow for a label-free detection of common plastic explosive materials, such as 2,4,6-trinitrotoluene (TNT), which is a leading example of nitroaromatic explosives. Results suggest that TNT concentrations as low as 10^{-9} M can be accurately detected using the described SERS substrates.

Acknowledgements

Financial support by the Program for Excellent Doctoral Thesis of Chinese Academy of Sciences, "Hundred Talents Project" of Chinese Academy of Sciences, and the National Basic Research Program of China (973 Program; No. 2010CB933600), NSFC (No. 20873138) is gratefully acknowledged.

References

[1] K.D. Smith, B.R. McCord, W.A. MacCrehan, K. Mount, W.F. Rowe, J. Forensic Sci. 44 (1999) 789–794.
[2] J.S. Yang, T.M. Swager, J. Am. Chem. Soc. 120 (1998) 5321–5322.
[3] S.J. Toal, W.C. Trogler, J. Mater. Chem. 16 (2006) 2871–2883.
[4] D. Gao, Z. Wang, B. Liu, L. Ni, M. Wu, Z. Zhang, Anal. Chem. 80 (2008) 8545–8553.
[5] W. Chen, N.B. Zuckerman, J.P. Konopelski, S. Chen, Anal. Chem. 82 (2010) 461–465.
[6] T. Carona, M. Guillemot, P. Montméat, F. Veignal, F. Perraut, P. Prené, F. Sereine-Spirau, Talanta 81 (2010) 543–548.
[7] Y. Jiang, H. Zhao, N. Zhu, Y. Lin, P. Yu, L. Mao, Angew. Chem. Int. Ed. 47 (2008) 8601–8604.
[8] N.P. Saravanan, S. Venugopalan, N. Senthilkumar, P. Santhosh, B. Kavita, H.G. Prabu, Talanta 69 (2006) 656–662.
[9] F. Wang, W. Wang, B. Liu, Z. Wang, Z. Zhang, Talanta 79 (2009) 376–382.
[10] M. Riskin, R.T. Vered, T. Bourenko, E. Granot, I. Willner, J. Am. Chem. Soc. 130 (2008) 9726–9733.
[11] E.R. Goldman, I.L. Medintz, J.L. Whitley, A. Hayhurst, A.R. Clapp, T. Uyeda, J.R. Deschamps, M.E. Lassman, H. Mattoussi, J. Am. Chem. Soc. 127 (2005) 6744–6751.
[12] K. Matsumoto, A. Torimaru, S. Ishitobi, T. Sakai, H. Ishikawa, K. Toko, N. Miura, T. Imato, Talanta 68 (2005) 305–311.
[13] M. Cerruti, J. Jaworski, D. Raorane, C. Zueger, J. Varadarajan, C. Carraro, S.W. Lee, R. Maboudian, A. Majumdar, Anal. Chem. 81 (2009) 4192–4199.
[14] H. Ko, V.V. Tsukruk, Small 4 (2008) 1980–1984.
[15] S.S.R. Dasary, A.K. Singh, D. Senapati, H. Yu, P.C. Ray, J. Am. Chem. Soc. 131 (2009) 13806–13812.
[16] H. Ko, S. Chang, V.V. Tsukruk, ACS Nano 3 (2009) 181–188.
[17] A. Kudelski, Talanta 76 (2008) 1–8.
[18] Y. Sun, L. Sun, B. Zhang, F. Xu, Z. Liu, C. Guo, Y. zhang, Z. Li, Talanta 79 (2009) 562–569.
[19] J.F. Li, Y.F. Huang, Y. Ding, Z.L. Yang, S.B. Li, X.S. Zhou, F.R. Fan, W. Zhang, Z.Y. Zhou, D.Y. Wu, B. Ren, Z.L. Wang, Z.Q. Tian, Nature 464 (2010) 392–395.
[20] S. Nie, S.R. Emory, Science 275 (1997) 1102–1106.
[21] H. Xu, J. Aizpurua, M. Käll, P. Apell, Phys. Rev. E 62 (2000) 4318–4324.
[22] Y. Fang, N.H. Seong, D.D. Dlott, Science 321 (2008) 388–392.
[23] H. Xu, M. Käll, Chemphyschem 4 (2003) 1001–1005.
[24] H. Wei, U. Håkanson, Z. Yang, F. Höök, H. Xu, Small 4 (2008) 1296–1300.
[25] H. Wei, F. Hao, Y. Huang, W. Wang, P. Nordlander, H. Xu, Nano Lett. 8 (2008) 2497–2502.
[26] A.D. Strickland, C.A. Batt, Anal. Chem. 81 (2009) 2895–2903.
[27] A. Kaminska, O.I. Agha, R.J. Forster, T.E. Keyes, Phys. Chem. Chem. Phys. 10 (2008) 4172–4180.
[28] M.L. Zhang, X. Fan, H.W. Zhou, M.W. Shao, J.A. Zapien, N.B. Wong, S.T. Lee, J. Phys. Chem. C 114 (2010) 1969–1975.

[29] L.H. Lu, A. Kobayashi, K. Tawa, Y. Ozaki, Chem. Mater. 18 (2006) 4894–4901.
[30] L.H. Lu, K.L. Ai, Y. Ozaki, Langmuir 24 (2008) 1058–1063.
[31] L.H. Lu, A. Eychmüller, Acc. Chem. Res. 41 (2008) 244–253.
[32] L.H. Lu, I. Randjelovic, R. Capek, N. Gaponik, J.H. Yang, H.J. Zhang, A. Eychmüller, Chem. Mater. 17 (2005) 5731–5736.
[33] L.H. Lu, R. Capek, A. Kornowski, N. Gaponik, A. Eychmüller, Angew. Chem. Int. Ed. 44 (2005) 5997–6001.
[34] L.H. Lu, A. Eychmüller, A. Kobayashi, Y. Hirano, K. Yoshida, Y. Kikkawa, K. Tawa, Y. Ozaki, Langmuir 22 (2006) 2605–2609.
[35] L. Gunnarsson, E.J. Bjerneld, H. Xu, S. Petronis, B. Kasemo, M. Käll, Appl. Phys. Lett. 78 (2001) 802–804.
[36] C.L. Haynes, R.P. Van Duyne, J. Phys. Chem. B 105 (2001) 5599–5611.
[37] A.G. Brolo, E. Arctander, R. Gordon, B. Leathem, K.L. Kavanagh, Nano Lett. 4 (2004) 2015–2018.
[38] B.H. Zhang, H.S. Wang, L.H. Lu, K.L. Ai, G. Zhang, X.L. Cheng, Adv. Funct. Mater. 18 (2008) 2348–2355.
[39] X.M. Zhao, B.H. Zhang, K.L. Ai, G. Zhang, L.Y. Cao, X.J. Liu, H.M. Sun, H.S. Wang, L.H. Lu, J. Mater. Chem. 19 (2009) 5547–5553.
[40] H. Wang, C.S. Levin, N.J. Halas, J. Am. Chem. Soc. 127 (2005) 14992–14993.
[41] D.A. Genov, A.K. Sarychev, V.M. Shalaev, A. Wei, Nano Lett. 4 (2004) 153–158.
[42] T. Ming, W. Feng, Q. Tang, F. Wang, L. Sun, J. Wang, C. Yan, J. Am. Soc. Chem. 131 (2009) 16350–16351.
[43] T. Ming, X. Kou, H. Chen, T. Wang, H.L. Tam, K.W. Cheah, J.Y. Chen, J. Wang, Angew. Chem. Int. Ed. 47 (2008) 9685–9690.
[44] L.H. Lu, H.S. Wang, S.Q. Xi, H.J. Zhang, J. Mater. Chem. 12 (2002) 156–158.
[45] L.H. Lu, A. Kobayashi, Y. Kikkawa, K. Tawa, Y. Ozaki, J. Phys. Chem. B 110 (2006) 23234–23241.
[46] C.J. Orendorff, A. Gole, T.K. Sau, C.J. Murphy, Anal. Chem. 77 (2005) 3261–3266.
[47] A.R. Tao, D.P. Ceperley, P. Sinsermsuksakul, A.R. Neureuther, P. Yang, Nano Lett. 8 (2008) 4033–4038.
[48] K.J.M. Bishop, C.E. Wilmer, S. Soh, B.A. Grzybowski, Small 5 (2009) 1600–1630.
[49] P. Kekicheff, H.K. Christenson, B.W. Ninham, Colloids Surf. 40 (1989) 31–41.
[50] D. Seo, J.C. Park, H. Song, J. Am. Chem. Soc. 128 (2006) 14863–14870.
[51] F. Kim, S. Connor, H. Song, T. Kuykendall, P. Yang, Angew. Chem. Int. Ed. 43 (2004) 3673–3677.
[52] H. Ko, S. Singamaneni, V.V. Tsukruk, Small 4 (2008) 1576–1599.
[53] B. Nikoobakht, M.A. El-Sayed, J. Phys. Chem. A 107 (2003) 3372–3378.
[54] M. Mulvihill, A. Tao, K. Benjauthrit, J. Arnold, P. Yang, Angew. Chem. Int. Ed. 47 (2008) 6456–6460.
[55] H.X. Xu, E.J. Bjerneld, M. Käll, L. Börjesson, Phys. Rev. Lett. 83 (1999) 4357–4360.
[56] J. Clarksona, W.E. Smitha, D.N. Batchelder, D.A. Smith, A.M. Coats, J. Mol. Struct. 648 (2003) 203–214.
[57] P.H.C. Camargo, M. Rycenga, L. Au, Y. Xia, Angew. Chem. Int. Ed. 48 (2009) 2180–2184.